ASIAN JOURNAL OF CIVIL ENGINEERING (BHRC) VOL. 16, NO. 2 (2015)
PAGES 219-233

NEW ALTERNATIVES FOR CONTINUITY PLATES IN I-BEAM TO BOX COLUMNS CONNECTIONS

H. Saffari[1*], A. A. Hedayat[2] and N. Soltani Goharrizi[3]
[1]Department of Civil Engineering, Faculty of Engineering, Shahid Bahonar University of Kerman, Kerman, Iran
[2]Department of Civil Engineering, Kerman Branch, Islamic Azad University, Kerman, Iran
[3]Department of Civil Engineering Science and Research Branch, Islamic Azad University, Isfahan, Iran

Received: 12 August 2014; **Accepted:** 15 October 2014

ABSTRACT

Due to the closed shape of box columns and difficult access to its inside for developing a reliable load path regarding rigid I-beam to box columns connections, in this study, some alternatives have been suggested to replace continuity plates. These alternatives are: two triangular plates, two rectangular plates and added stiff web. To evaluate the efficiency of these suggested alternatives, using ANSYS software, several beam-column connections in each alternative have been modeled. Based on the finite element results the behavior of I-beam connection to steel box column has been studied. Then the effects of suggested stiffeners on connection stiffness, strength and ductility have been investigated. The results showed that each of the suggested methods might be a good alternative for rigid connection with internal uniform continuity plates. However specimens of additional stiffened webs achieved highest connection strength and ductility.

Keywords: Panel zone; moment resisting connections; box columns; continuity plates.

1. INTRODUCTION

Three main parameters in steel moment resisting connection (MRC) design are; stiffness, strength and ductility. The response of the beam-to-column connections is strongly affected by the panel zone. Wide experimental and analytical studies have been carried out in order to examine the behavior of panel zone [1,2,3]. Northridge (1994) and Kobe (1995) earthquakes showed that excessive shear distortions could create brittle ruptures at the welds of beam-to-column connection [4,5,6]. The results obtained from these Earthquakes have reflected in the subsequent changes proposed to the design approach in the American and

*E-mail address of the corresponding author: hsaffari@uk.ac.ir (H. Saffari)

European codes. AISC prequalified connections can be used for columns if horizontal continuity plates are used inside the column. The use of internal horizontal continuity plates as thick as the beam flange plates or stiffeners has been emphasized by FEMA355-D [7], to provide good seismic performance for beam-to-column connections [8]. Some applicable method for calculating shear strength of panel zone in beam-to-column connections has been presented [7,8,9,10]. Continuity plates are welded to the column web and flange at the level of tension and compression beam flanges. Performing of these plates in connection of I-beams to wide flange columns is easy and possible. Large flexural and torsional stiffness and high strength about any axis of box-shape columns make these sections more efficient than conventional wide flange sections in flexural and compression members such as beam-columns. Although box-columns have these advantages, but, as the section is closed, welding of the forth side of the continuity plate to the column is not easily done. Finding a proper beam to column connection is still under investigation. Different types of external stiffeners, including triangular plates, T- and angle-stiffeners, were used to provide a proper load path between the I-beam and the box-column [3,11,1213]. A new beam to box-column moment connection called diagonal through-plate connection has been presented in references [14,15] to eliminate the horizontal continuity plates.

The purpose of this study is to suggest some suitable alternative for internal, uniform continuity plates in moment resisting beam to steel box-columns connections. These alternatives are: triangular and rectangular continuity plates and added stiff web. Using finite element method several beam-column connections in each alternative have been modeled and analyzed. Then the effects of suggested stiffeners on connection stiffness, strength and ductility for different beam length-beam depth ratios have been investigated.

2. PROPOSED ALTERNATIVES FOR CONTINUTY PLATES

In the following, three alternatives are suggested for continuity plates:

1- Using of two triangular plates at the level of each top and bottom beam flanges instead of internal uniform continuity plate. In this case the box-column is made by joining two angle-shape parts where triangular continuity plates are welded to each part separately (Fig. 1).

2- Using of two rectangular plates at the level of each top and bottom beam flanges instead of internal uniform continuity plate. In this case the box-column is made by joining two channel-shape parts where the rectangular continuity plates are welded to each part separately (Fig. 2).

3- Using of extra reinforced web inside the column, (Fig. 3).

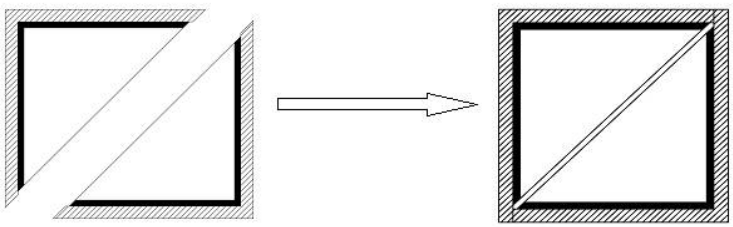

Figure 1. Triangular couple plates used in up and down flanges

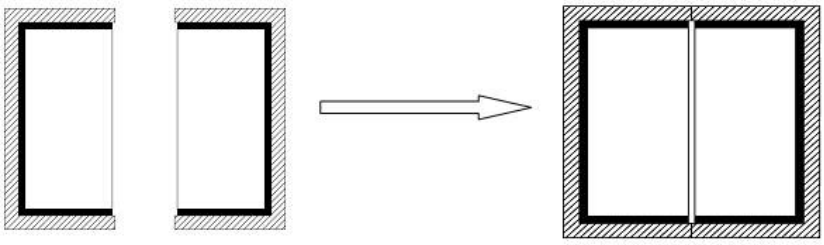

Figure 2. rectangular couple plates used as an alternative in up and down flanges

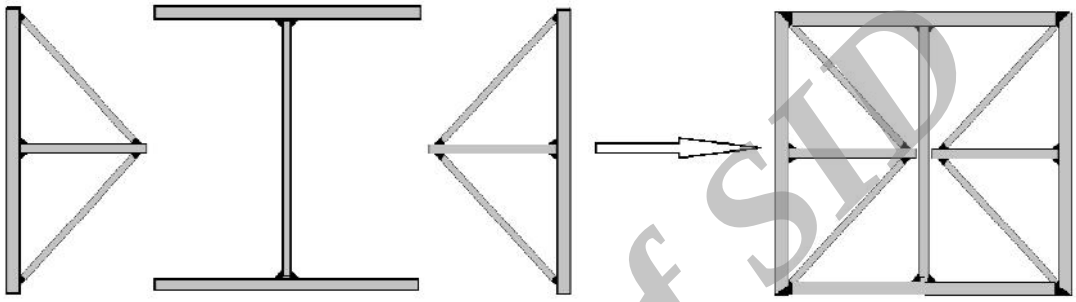

Figure 3. reinforced extra web inside the column

3. FINITE ELEMENT MODEL

Finite element models were created using the general purpose finite element program ANSYS-12 [16]. In finite element models, both welds and base metals were modeled using shell elements and the associated material property was defined for each one. SHELL43 was used to model weld and column plates whereas SHELL181 was used to model the beam plates. SHELL43 and SHELL181 are one-layer four-node and multi-layer eight-node shell elements respectively. These elements have six degrees of freedom at each node and all of them have plasticity, large deflection, and large strain capabilities. In the case of using SHELL181, each element was separated into five layers across the thickness. The number of layers was selected based on the finite element study carried out by Gilton and Uang [17]. To perform material nonlinearity analyses, plasticity behavior was based on the von-Mises yielding criteria and the associated flow rule. Isotropic hardening was assumed for the monotonic analysis, whereas kinematic hardening was assumed for the cyclic analysis as used by Mao et al. and Ricles et al. [18,19]. A bilinear material response was used for based metals whilst for weld metals; a multi-linear material response based on material property given in references [18,19] was used. The monotonic analyses were conducted by applying a monotonic vertical displacement load to the beam tip until achieving more than 4% total rotation at column web center, whereas the load history recommended in FEMA350 [19] was utilized for cyclic analyses. When applied loads are in the vertical direction only, then the out-of-plane deformations (normal to the web) may not occur. Therefore, in order to ensure that buckling occurs when the model becomes unstable, the imperfect model was used to analyses under cyclic or monotonic loadings. In this study, in order to determine the imperfect model, first the buckling mode shapes were computed in a separate buckling

analysis and then were implemented to perturb the original perfect geometry of the model as it was in [21,22,23,24,25,26].

In order to verify the accuracy of finite element modeling, a pretested box-column to I-beam connection, specimen W08-L1A of Cheng et al. [27], (Fig. 4), was modeled using the procedure mentioned in previous paragraph. Fig. 5 shows the finite element mesh of this specimen. Experimental and numerical results of this specimen were compared in terms of beam tip load and beam rotation. Fig. 6 shows this comparison. The initial stiffness, maximum load achieved at the peak of the beam tip displacement and post-elastic envelopes under under upward loadings were well matched for the finite element model and the test specimen. However, when loads become downward a minor mismatch can be seen between the two curves at large rotations. Therefore, it might be concluded that the analytical results are in good agreement with experimental results.

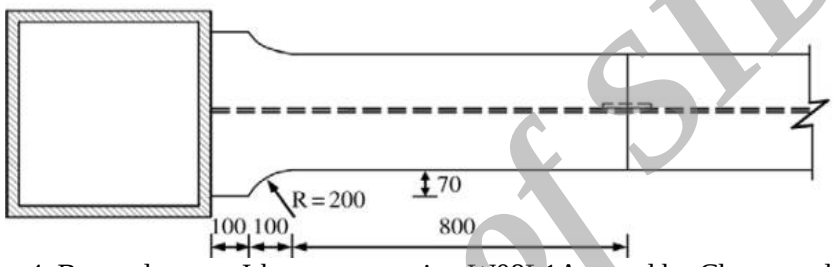

Figure 4. Box-column to I-beam connection W08L1A tested by Cheng et al. [24]

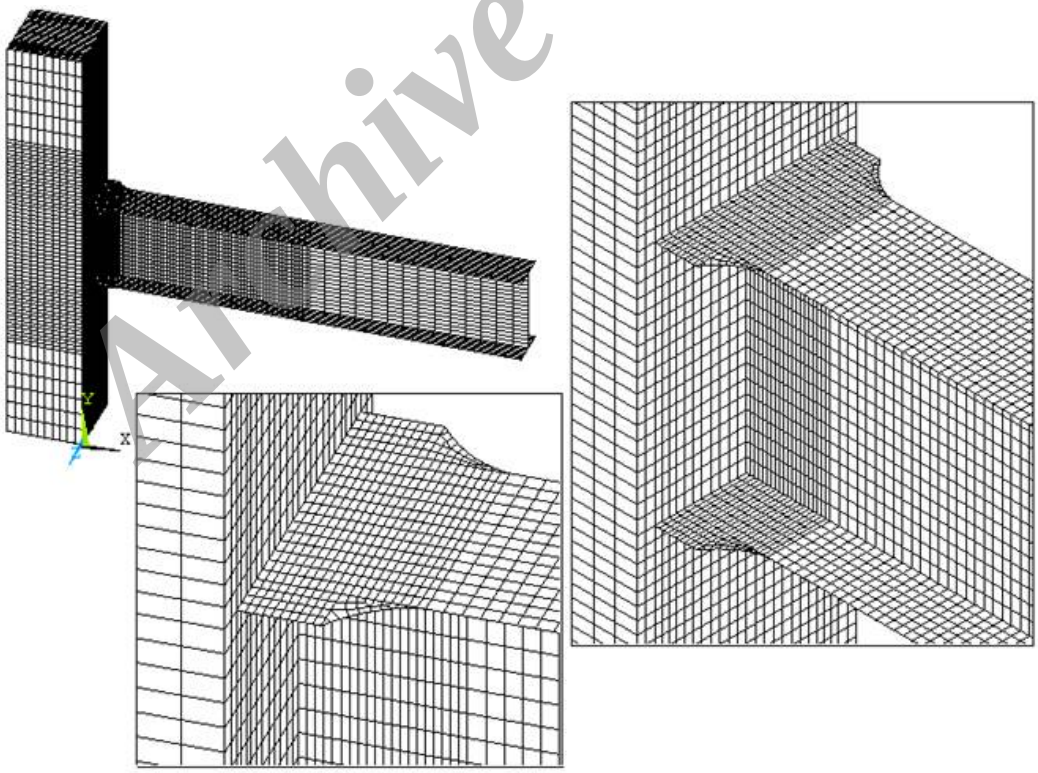

Figure 5. Finite element mesh of specimen W08L1A pretested by Cheng et.al [24]

4. PARAMETRIC STUDY

In this study, the proposed stiffener configurations (Figs. 1 to 3) were applied to each specimen of B-SAC and B-SPE group specimens (Table 1), which represent different beam heights from 450 mm to 912 mm. B-SAC and B-SPE specimens comprised of a built-up box-shape column and a wide flange I-shape beam. The connection details of these specimens are exactly the same as SAC and SPE specimens presented in [21,28] respectively (i.e., all specimens have post-Northridge connection detail) except that the box-shape columns have been used instead of I-shape columns. Box columns were designed as such to have exactly the same capacity as that of I-shape columns used in SAC and SPE specimens presented in [21,28]. All the designs have been developed using AISC2010 specification [29]. These specimen sizes were chosen since they may be good representatives of the conventional specimen sizes, small, medium and large [28].

Table 1: Details of B-SPE and B-SAC group connections

Specimen	Type	Section	fy (Mpa)
B-SAC7	Beam	W36*150	250
	Column	BOX420*400*45*25	345
B-SPE7	Beam	W36*170	250
	Column	BOX420*400*45*25	345
B-SAC5	Beam	W30*99	250
	Column	BOX405*405*30*15	345
B-SPE5	Beam	W36*116	250
	Column	BOX405*405*30*15	345
B-SAC3	Beam	W24*68	250
	Column	BOX375*375*20*10	345
B-SPE3	Beam	W24*84	250
	Column	BOX375*375*20*10	345
B-SPE2	Beam	W18*55	250
	Column	BOX305*305*20*10	345
B-SPE1	Beam	W18*46	250
	Column	BOX305*305*20*10	345

The effects of each proposed continuity plate on the initial rotational stiffness, strength and ductility of each B-SAC and B-SPE specimen were compared to those of specimens with the conventional uniform continuity plates, where these plates were either welded to the column flange plates from four sides (Fig. 7, specimen B0) or from three sides depends on the orientation of the beam (specimens B1 to B3, Fig. 7). In B4 specimen, the box column is a combination of two angle shape parts, to which triangular continuity plates were welded whilst in the B5 and B6 specimens, the box column is made of two channel shape parts, to which rectangular continuity plates were welded. In B7 and B8 specimens, a reinforced web with a height of 2 times that of the beam overall depth was used instead of the continuity

plates in the box column (Fig. 7). These proposed alternatives are intended to make easy the fabrication of built-up box columns by removing the use of conventional continuity plates where these plates are welded to the column flange plates from four sides which their fabrication are relatively difficult.

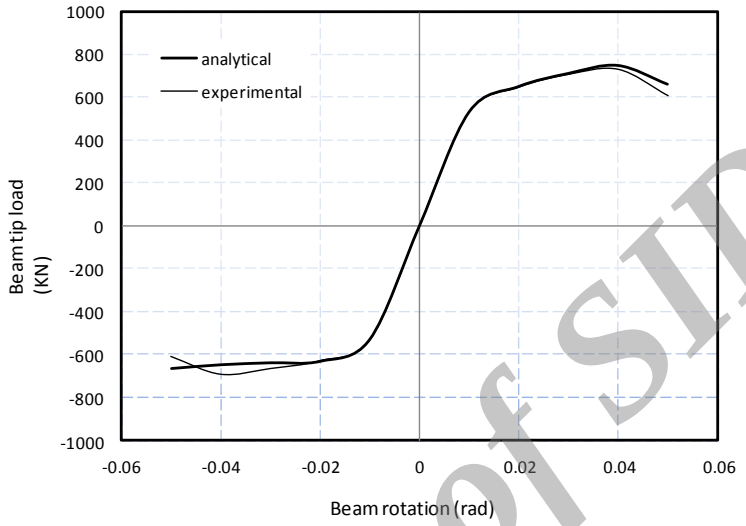

Figure 6. Comparison between analytical and experimental results of specimen W08L1A [24]

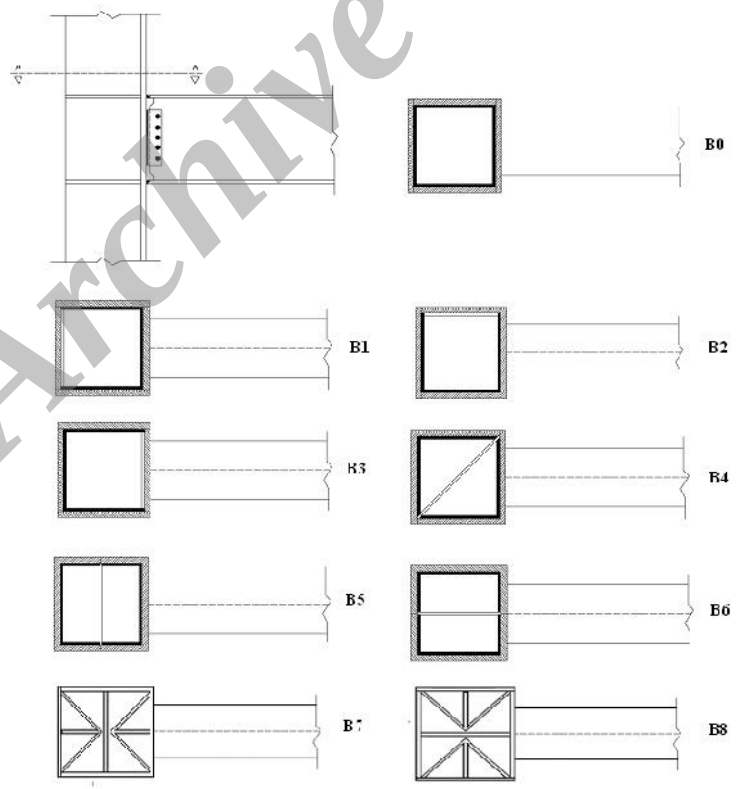

Figure 7. Alternatives for continuity plates

5. ANALYTICAL RESULTS

5.1 Failure criteria and failure modes

It is well known that in the welded connections at a region near the column face the classic beam theory is invalid [22,30,31,32,33]. In this region, shear stresses are at a maximum level near the column flanges, especially at the weld access hole (WAH) region. The combination of shear stresses and normal stresses at the beams flanges near the column face, promotes the brittle fracture of welded connections. Hence, it seems that the use of von-Mises strains might be more appropriate than normal strains to estimate the failure of material near the column face and even at a region away from the column face. Hence in this study as a sample finite element model of B1-SAC5 has been shown in Fig. 8 and the failure criterion was defined as follows:

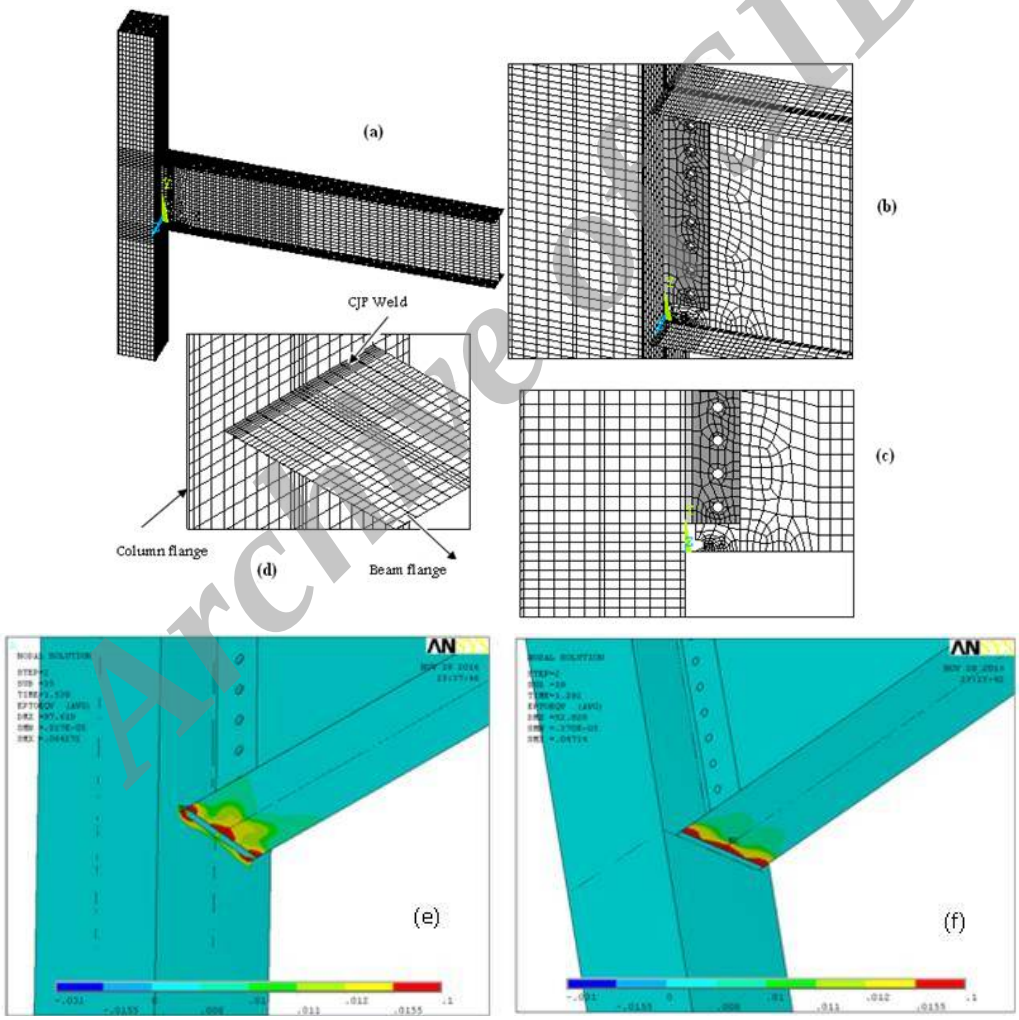

Figure 8. finite element model B1-SAC5 (a) whole illustration of beam and column (b) illustration of shear tab (c) illustration of bolt holes and weld access hole (d) welding modeling using shell elements (e) Fracture of connection at column flange (f) Fracture of connection at beam flange

Connection fracture occurs when von-Mises strains at the half or entire beam or column flange widths (depends on connection type) at column face level exceed the stain associated with the ultimate strength of the beam or column flange materials, based on the material properties reported by Lee et al. 2000 (Fig. 8). However, to ensure for estimating of the connection failure time, in some models, Birth and Death characteristics of elements in ANSYS software was used.

5.2 Effects of proposed alternatives on the normalized Von-Mises strains

Figs. 9(a) and 9(b) show the distribution of the normalized Von-Mises strains of B-SAC7 specimens B0, B4, B6 and B7 under monotonic upward loading at 2 and 4 percent total rotation respectively. Total rotation was measured at the column web center. Normalized strains were obtained at the most critical location of a post-Northridge connection, WAH region, by dividing the measured Von-Mises strain by the yield strain of the beam flange material. As these Figs. show the level of strains at the beam flange edges are much more than those which were measured at the beam flange center, indicating that the connection fracture initiates from the beam flange edge.

As Figs. 9(a) and 9(b) show, at two and four percent total rotations, the level of Von-Mises strains for specimens B0 and B6 are approximately same, indicating achieving same fracture time and perhaps same ductility (total rotation). Comparing specimen B7 and B0 indicate that the use of additional stiffened webs can cause a reduction in the level of von-Mises strains at beam flange at WAH region which is in contrast with the use of B6 configuration. Hence, from the ductility point of view it might be concluded that, among all alternatives, the B7 configuration is the best. Similar behaviors were also observed for all other SAC and SPE specimens.

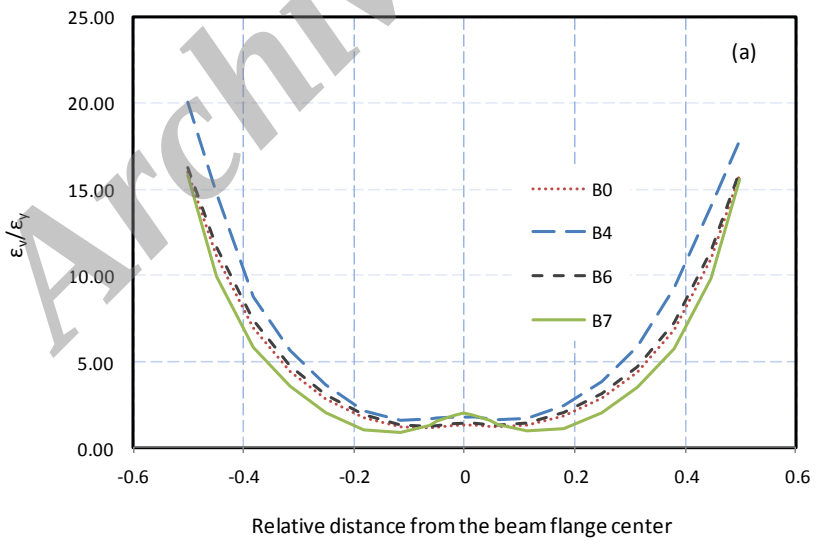

Figure 9a. Normalized Von-Misses strain distributions for whole beam flange width at weld access hole region of B-SAC7 specimens B0,B4,B6 and B7 at 2 percent total rotation

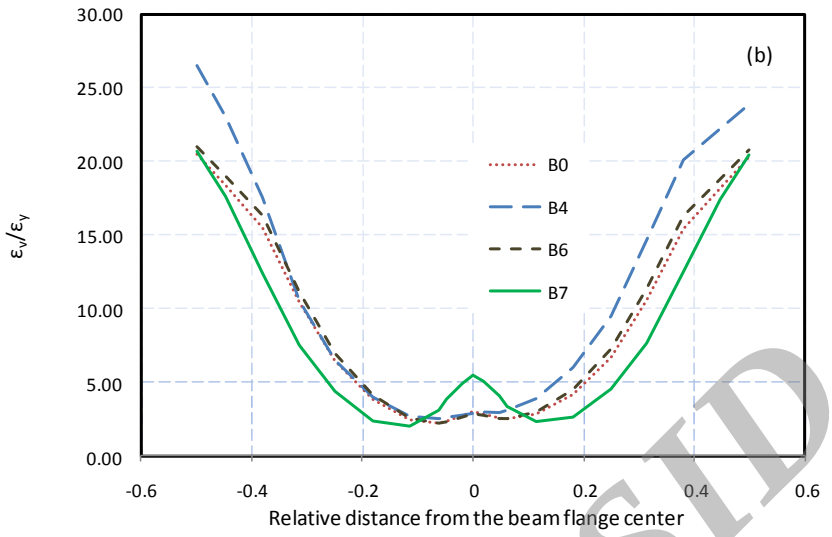

Figure 9b. Normalized Von-Misses strain distributions for whole beam flange width at weld access hole region of B-SAC7 specimens B0,B4,B6 and B7 at 4 percent total rotation

5.3 Effects of proposed alternatives on the secondary flexural stresses

Fig. 10 shows the distribution of normalized normal stresses at the surface of bottom beam flange as a function of distance from the face of the column at 2 percent total rotation (story drift) for B-SAC7 specimens. Normal stresses and the distance from the column face were normalized with respect to the yield stress of beam flange material and the beam overall depth respectively. These distributions are presented at beam flange edge which is the critical location of a box column. As this Figure shows the distribution of normalized strains are linear and follow the classical beam theory beyond about 10 percent of the beam overall depth from the column face. However, at the column face, normalized strains suddenly increased. This increase is due to the secondary flexural stresses which were resulted from transfer of remarkable part of shear forces via the beam flanges (which is in contrast with the classical beam theory).

The effect of each alternative on the peak of normal strain was different. Using B4 and B6 configurations caused a 22.8 percent and 2.3 percent increase in the amount of maximum strain of B0 specimen respectively. However, for B7 specimen, there was 2.3 percent reduction in the amount of strain in the peak compared to B0 specimen.

5.4 Effects of proposed alternatives on the connection strength, ductility and initial rotational stiffness

Among all B-SAC and B-SPE specimens, Fig. 11 compares the moment-rotation curves of B-SAC7 specimens B0 to B8. Table 2 summarizes strength, ductility and normalized initial rotational stiffness of all B-SAC and B-SPE specimens. In this table total rotations were calculated at the column web center and failure moments were normalized with respect to the beam plastic moment in each specimen. To see the effect of each proposed alternative on the connection initial rotational stiffness, these values were normalized with respect to the initial rotational stiffness of specimen B0.

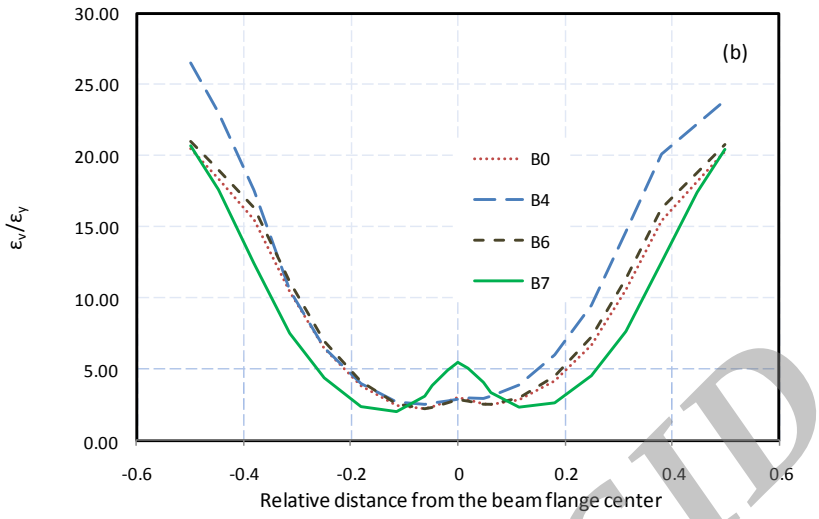

Figure 10. Normalized normal strain distributions for B-SAC7 specimens B0,B4,B6 and B7 at the beam flange edge at 2 percent total rotation

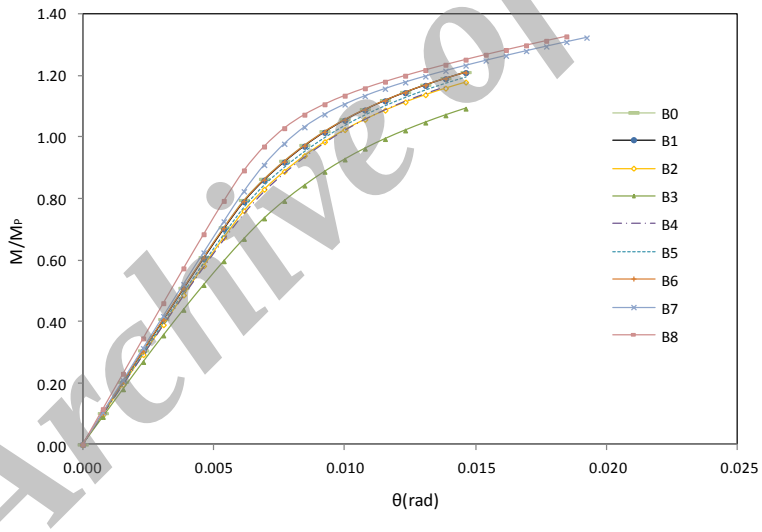

Figure 11. Moment-rotation curves for all B-SAC7 specimens

Table 2: Finite element results of all B-SAC and B-SPE specimens

Specimen type	Beam section	Column section	Specimen	Total rotation θ(%)	Failure moment M(kN.m)	M/MP	Normalized initial rotational stiffness
B-SAC7	W 36*150	BOX420*400*45*25	B0	1.46	2882.41	1.21	1
			B1	1.46	2878.33	1.21	0.98
			B2	1.46	2805.01	1.18	0.94
			B3	1.46	2599.5	1.09	0.88
			B4	1.38	2768.19	1.16	0.94

B-SPE7	W36*170	BOX420*400*45*25	B5	1.46	2841.94	1.19	0.96
			B6	1.46	2878.4	1.21	0.98
			B7	1.92	3149.27	1.32	1.01
			B8	1.85	3158.78	1.33	1.12
			B0	1.38	3146.84	1.15	1
			B1	1.38	3140.32	1.15	0.99
			B2	1.38	3114.5	1.14	0.97
			B3	1.23	2579.79	0.94	0.86
			B4	1.38	3046.01	1.11	0.94
			B5	1.38	3090.56	1.13	0.97
			B6	1.38	3141.83	1.15	0.99
			B7	1.92	3502.94	1.28	1.01
			B8	1.85	3525.28	1.29	1.12
B-SAC5	W 30*99	BOX405*405*30*15	B0	1.38	1415.17	1.11	1
			B1	1.38	1409.21	1.1	0.99
			B2	1.38	1373.97	1.07	0.94
			B3	1.31	910.474	0.71	0.7
			B4	1.38	1219.05	0.95	0.88
			B5	1.38	1360.97	1.06	0.96
			B6	1.38	1406.33	1.1	0.99
			B7	2.46	1688.36	1.32	0.96
			B8	2.23	1656.77	1.3	1.01
B-SPE5	W 30*116	BOX405*405*30*15	B0	1.46	1731.35	1.12	1
			B1	1.46	1728.15	1.12	0.99
			B2	1.46	1669.39	1.08	0.94
			B3	1.08	903.06	0.58	0.7
			B4	1.38	1521.02	0.98	0.9
			B5	1.46	1670.17	1.08	0.96
			B6	1.46	1726.16	1.11	0.99
			B7	1.92	1847.43	1.19	0.93
			B8	2.23	1942.25	1.25	0.99
B-SAC3	W 24*68	BOX375*375*20*10	B0	1.54	798.75	1.1	1
			B1	1.54	797.62	1.1	0.99
			B2	1.54	769.98	1.06	0.93
			B3	1.23	377.18	0.52	0.6
			B4	1.54	716.9	0.99	0.9
			B5	1.54	765.6	1.06	0.95
			B6	1.46	781.05	1.08	0.99
			B7	2.46	905.35	1.25	0.94
			B8	2.69	915.699	1.26	0.93
B-SPE3	W 24*84	BOX375*375*20*10	B0	1.62	1023.43	1.12	1
			B1	1.62	1022.15	1.11	1
			B2	1.69	993.49	1.08	0.93
			B3	1.08	380.58	0.41	0.57
			B4	1.62	907.3	0.99	0.9
			B5	1.62	1001.17	1.09	0.97
			B6	1.62	1020.83	1.11	1
			B7	1.62	968.932	1.06	0.9
			B8	1.77	969.226	1.06	0.89

B-SPE2	W 18*55	BOX305*305*20*10	B0	2	524.02	1.14	1
			B1	2	523.39	1.14	0.99
			B2	2	507.78	1.11	0.93
			B3	1.31	237.8	0.52	0.65
			B4	1.85	466.48	1.02	0.9
			B5	2	512.54	1.12	0.96
			B6	2	523.1	1.14	0.99
			B7	3.92	601.08	1.31	0.91
			B8	4.15	609.28	1.33	0.94
B-SPE1	W 18*46	BOX305*305*20*10	B0	1.69	379.603	1.02	1
			B1	1.69	378.99	1.02	0.99
			B2	1.69	370.407	1	0.94
			B3	1.31	190.737	0.51	0.6
			B4	1.77	360.369	0.97	0.9
			B5	1.69	372.756	1	0.96
			B6	1.69	378.486	1.02	0.99
			B7	3.08	446.948	1.2	0.93
			B8	2.85	436.311	1.17	0.94

Comparing the results of specimens B0 to B3 for all B-SAC and B-SPE specimens shows that specimens B3 in which the continuity plate is not welded to the column flange on the side where the beam is connected to the column, have the lowest strength, ductility and initial rotational stiffness among all specimens. Finite element results showed that these specimens failed due to the column flange fracture at low level of connection total rotation. The minimum values for normalized strength (M/MP) and normalized stiffness for B3 specimens were observed for B-SPE3 specimens which were 0.41 and 0.57 respectively. These very low values indicate that in a rigid connection, the continuity plate should be welded to the column flange on the side where the beam is connected unless this connection must be evaluated as a semi-rigid connection. Specimens B0, B1 and B2 approximately showed same behavior however for all cases B1 specimens showed better connection performance (strength, ductility and initial rotational stiffness).

In B4 specimen connections, due to the triangular shape of continuity plates which caused an unsymmetrical strain distribution on the entire column flange width, column flange fracture initiated on the side shown in Fig. 12, simultaneously with the beam flange fracture. But, finally, the connection failed due to the beam flange fracture. In these connections the achieved ductility was not so much different from that of B0. But there was a reduction in the connection strength and rotational stiffness when compared with B0 specimens. This reduction for strength was in average 9 percent and in the worst case was 14.4 percent. Average reduction in connection rotational stiffness was 9 percent and in the worst case was 12 percent.

Comparing specimens B5 and B6 with B0 shows that there is no difference in achieving connection ductility. However there were observed an unremarkable reduction in the connection rotational stiffness and strength. For B5 specimens these reductions for achieving connection strength and initial rotational stiffness were about 4 percent and 2.7 percent respectively. B6 specimens even showed higher performance. Reduction in the achieved connection strength and initial rotational stiffness for B6 specimens in compare to B0

specimens were in average 0.6 percent and 1 percent respectively. Both B5 and B6 specimens failed due to the beam flange fracture at weld access hole region.

Among all proposed alternatives, B7 and B8 specimens showed the highest performance. Using B7 configuration, in average caused 52 percent and 10.8 percent increase in the connection ductility and strength respectively when they were compared to B0 specimens. However, there was only 5 percent reduction in the connection initial rotational stiffness. Specimens of B8 configuration even showed higher performance. For these specimens increase in the connection ductility and strength was in average 54.2 and 11.5 percent respectively. While reduction in the connection initial rotational stiffness was only 1 percent. Both B7 and B8 specimens failed due to the beam flange facture at weld access hole region.

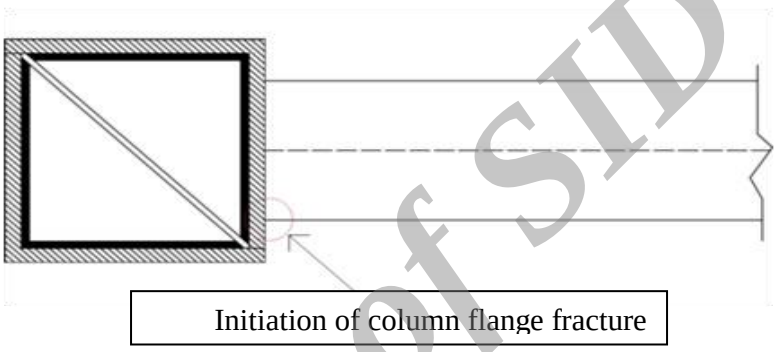

Figure 12. Location of fracture initiation of B4 specimens

6. CONCLUTION

Due to the closed shape of box columns access to the inside of the column is difficult. In this case welding the continuity plates to the column flanges from four sides is relatively difficult and costly. Hence, this study was aimed to introduce some alternatives for continuity plates to reduce their difficulties during fabrication while connection strength, ductility and initial rotational stiffness remain unchanged. The proposed alternatives were using two triangular continuity plates (specimen B4), two rectangular continuity plates (specimen B5 and B6) and using additional stiffened webs at the connection area (specimens B7 and B8). Parametric studies were done on post-Northridge connections of beams with different height (450 mm to 912mm) and different flange thickness. Finite element results showed that:

1. In the case of using conventional continuity plate in a rigid connection, the continuity plate should be welded to the column flange on the side where the beam is connected unless this connection must be evaluated as a semi-rigid connection.

2. Among connections of triangular, rectangular and additional stiffened webs, use of triangular plates led to the achievement of minimum performance (connection performance was less than the one of conventional continuity plates, specimen B0) while specimens of rectangular plates (B5 and B6 specimens) achieved same performance as specimen B0. Specimens B7 and B8, which used additional stiffened webs attained highest performance, their strength and ductility were in average 11.5 and 54.2 percent higher than specimen B0 respectively.

Hence it might be concluded that among the proposed methods, the use of additional

stiffened webs is the best alternative for continuity plates. It should be noted that even the use of additional stiffened webs did not lead to the achievement of minimum required ductility of a connection (4 percent total rotation). Therefore, as reported by all researchers beam end configuration must be modified to enhance connection ductility (e.g. reducing the beam section at vicinity of the column, using RBS connections).

REFERENCES

1. Krawinkler H, Bertero VV, Popov EP. Inelastic behaviour of steel beam-to-column subassemblages, Report No EERC-71/7, Earthquake Engineering Research Center, University of California, 1971.
2. Bertero VV, Krawinkler H, Popov EP. Further studies on seismic behavior of steel beam-column subassemblages, Report No. EERC-73/27. Berkeley, California: Earthquake Engineering Research Center, University of California, 1973.
3. Popov EP. Panel zone flexibility in seismic moment joints, *Journal of Constructional Steel Research*, **8**(1987) 91-118.
4. Mahin SA, Hamburger RO, Malley JO. An integrated program to improve the performance of welded steel frame buildings, *Proceedings of 11th WCEE World Conference Earthquake Engineering*, Acapulco, Mexico, Elsevier Science Ltd, 1996, Paper No. 1114.
5. Kunnath SK, Malley JO. Advances in seismic design and evaluation of steel moment frames: recent findings from FEMA/SAC Phase II Project, *Journal of Structural Engineering ASCE*, 2002, **128**(2002) 415-9.
6. AISC/ANSI 358-05. Prequalified connections for special and intermediate steelmoment frames for seismic applications specification, Chicago (IL), American Institute of Steel Construction, Inc. 2005.
7. FEMA-355D, State of the art report on connection performance, Washington, DC, Federal Emergency Management Agency, 2000.
8. De Luca A, Mele E, Brandonisio G. Shear strength of panel zone in beam-to- column connections, *Journal of Constructional Steel Research*, **26**(2011) 77-89.
9. Ting LC, Shanmugam NE, Lee SL. Box-column to I-beam connections with external stiffeners, *Journal of Constructional Steel Research*, **18**(1991) 209-26.
10. Saffari H, Hedayat AA, Goharrizi NS. Suggesting double-web I-shaped columns for omitting continuity plates in a box-shaped column, *Steel and Composite Structures*, **6**(2013) 585-603
11. Shanmugam NE, Ting LC, Lee SL. Behavior of I-beam to box-column connections stiffened externally and subjected to fluctuating loads, *Journal of Constructional Steel Research*, **20**(1991) 129-48.
12. Ting LC, Shanmugam NE, Lee SL. Design of I-beam to box-column connections stiffened externally, *Engineering Journal*, **30**(1993) 141-9.
13. Lee SL, Ting LC, Shanmugam NE. Use of external t-stiffners in box-column to I-beam connections, *Journal of Constructional Steel Research*, **26**(1993) 77-98.
14. Mirghaderi SR, Torabian S, Keshavarzi F. I-beam to box-column connection by a vertical plate passing through the column, *Engineerring Structures*, **32**(2010) 2034-48.

15. Torabian S, Mirghaderi SR, Keshavarzi F. Moment-connection between I-beam and built-up square column by a diagonal through plate, *Journal of Constructional Steel Research*, **70**(2011) 385-401.
16. ANSYS user manual. ANSYS, Inc, 2007.
17. Gilton CS, Uang CM. Cyclic response and design recommendations of weak-axis reduced beam section moment connections, *Journal of Structural Engineering*, **128**(2002) 452-63.
18. Mao C, Ricles J, Lu L, Fisher J. Effect of local details on ductility of welded moment connections, *Journal of Structural engineering*, **127**(2001) 1036-44.
19. Ricles JM, Mao C, Lu LW, Fisher JW. Ductile details for welded unreinforced moment connections subject to inelastic cyclic loading, *Engineering Structures*, **25**(2003) 667-80.
20. FEMA 350, Recommended Seismic Design Criteria for New Steel Moment-Frame Buildings, Washington, DC, Federal Emergency Management Agency, 2000.
21. Hedayat AA, Celikag M. post-Northridge connection with modified beam end configuration to enhance strength ductility, *Journal of Constructional Steel Research*, **65**(2009) 1413-30.
22. Hedayat AA, Celikag M. Wedge Design: A reduced beam web (RBW) connection for seismic regions, *Advances in Structural Engineering*, **13**(2009) 263-90.
23. Hedayat AA, Saffari H, Mousavi M. Behavior of steel reduced beam web (RBW) connections with arch-shape cut, *Advances in Structural Engineering*, **16**(2013) 1645.
24. Saffari H, Hedayat AA, Nejad MP. Post-Northridge connections with slit dampers to enhance strength and ductility, *Journal of Constructional Steel Research*, **80**(2013) 138-52.
25. SAC/BD-00/27. Cover-Plate and Flange-Plate reinforced steel-moment resisting connections, Kim T, Whittaker AS, Gilani AS, Bertero VV, Takhirov SM.
26. Moslehi Tabar A, Deylami A. Instability of beams with reduced beam section moment connections emphasizing the effect of column panel zone ductility, *Journal of Constructional Steel Research*, **6**(2005) 1475-91.
27. Cheng CC, Chun CL, Chieh HL. Ductile moment connections used in steel column-tree moment-resisting frames, *Journal of Constructional Steel Research*, **62**(2006) 793-801.
28. Lee H, Stojadinovic B, Goel SC, Margarian AG, Choi J, Wongkaew A, et al. Parametric Tests on Unreinforced Connections. SAC/BD-00/01, Volume I – Final Report, 2000.
29. ANSI/AISC 360-10, Specification for Structural Steel Buildings, American Institute of Steel Construction, 2010.
30. Hedayat AA, Celikag M. Fracture moment and ductility of welded connection, *Proceedings of the Institution of Civil Engineers Structures and Buildings*, **162**(2009) pp. 405-18.
31. Lee CH, Yoon TH. Analytical re-examination of shear transfer in welded steel moment connection, *Proceedings of the 1st Japan–Korea Joint Seminar on Earthquake Engineering for Building Structures*, **1**(1999) pp. 119-28.
32. Mansouri I, Saffari H. A new steel panel zone model including axial force for thin to thick column flanges, *Steel and Composite Structures*, **16**(2014) 417-36.
33. Cheol HL. Review of force transfer mechanism of welded steel moment connections, *Journal of Constructional Steel Research*, **62**(2006) 695-705.